Aerobic respiratory chain of *Escherichia coli* is not allowed to work in fully uncoupled mode

Vitaliy B. Borisov[a,1], Ranjani Murali[b,1], Marina L. Verkhovskaya[c], Dmitry A. Bloch[c], Huazhi Han[b], Robert B. Gennis[b], and Michael I. Verkhovsky[c,2]

[a]Belozersky Institute of Physico-Chemical Biology, Lomonosov Moscow State University, Moscow 119991, Russia; [b]Department of Biochemistry, University of Illinois, Urbana, IL 61801; and [c]Helsinki Bioenergetics Group, Institute of Biotechnology, University of Helsinki, PB 65 (Viikinkaari 1), FI-00014 Helsinki, Finland

Edited* by Pierre A. Joliot, Institut de Biologie Physico-Chimique, Paris, France, and approved August 11, 2011 (received for review May 26, 2011)

***Escherichia coli* is known to couple aerobic respiratory catabolism to ATP synthesis by virtue of the primary generators of the proton motive force—NADH dehydrogenase I, cytochrome bo_3, and cytochrome *bd*-I. An *E. coli* mutant deficient in NADH dehydrogenase I, bo_3 and *bd*-I can, nevertheless, grow aerobically on nonfermentable substrates, although its sole terminal oxidase cytochrome *bd*-II has been reported to be nonelectrogenic. In the current work, the ability of cytochrome *bd*-II to generate a proton motive force is reexamined. Absorption and fluorescence spectroscopy and oxygen pulse methods show that in the steady-state, cytochrome *bd*-II does generate a proton motive force with a H^+/e^- ratio of 0.94 ± 0.18. This proton motive force is sufficient to drive ATP synthesis and transport of nutrients. Microsecond time-resolved, single-turnover electrometry shows that the molecular mechanism of generating the proton motive force is identical to that in cytochrome *bd*-I. The ability to induce cytochrome *bd*-II biosynthesis allows *E. coli* to remain energetically competent under a variety of environmental conditions.**

Aerobic bacteria produce ATP via (*i*) oxygen-independent, substrate-level phosphorylation in glycolysis and the Krebs cycle, or (*ii*) oxidative phosphorylation, in which the electron flow, through the aerobic respiratory electron transport chain, generates a proton motive force ($\Delta p^{\%}$) which, in turn, drives the ATP synthase. The proton motive force ($\Delta p^{\text{out-in}}$, where it is specified that the gradient is measured "outside-minus-inside") is equivalent to the transmembrane electrochemical proton gradient and has chemical ($\Delta \text{pH}^{\text{out-in}}$) and electrical ($\Delta\Psi^{\text{out-in}}$) components. At 298 K, in mV units,

$$\Delta p^{\text{out-in}} = \Delta\Psi^{\text{out-in}} - 59\Delta \text{pH}^{\text{out-in}}$$

For bacteria, such as *Escherichia coli*, grown at neutral pH, the major component of the proton motive force is $\Delta\Psi^{\text{out-in}}$, which is positive outside and typically has a value in the range of 100 to 180 mV. Bacteria usually possess branched respiratory chains in which the different components are induced to allow the cells to adapt to various environmental conditions (1). One of the parameters that depends on the composition of the respiratory chain is the "bioenergetic efficiency," which can be defined as number of charges driven across the membrane per electron used to reduce oxygen to water, (q/e^-). In the *E. coli* respiratory chain, the net charge transfer across the membrane is equal to the number of protons released into the periplasm (H^+/e^-), which can be measured.

The aerobic respiratory chain of *E. coli* (Fig. 1) contains three enzymes that are known to generate a proton motive force: (*i*) the proton-pumping NADH:quinone oxidoreductase NADH dehydrogenase I (NDH-I) ($H^+/e^- = 2$) (2); (*ii*) cytochrome bo_3 ($H^+/e^- = 2$) (3), the proton-pumping oxygen reductase that is a member of the superfamily of heme-copper oxidoreductases (4–7); and (*iii*) cytochrome *bd*-I, which is unable to pump protons but generates a proton motive force by transmembrane charge separation resulting from utilizing protons and electrons originating from opposite sides of the membrane to generate water ($H^+/e^- = 1$) (5, 8–11). In addition, there are a number of substrate dehydrogenases that are not electrogenic, including the nonelectrogenic NADH:quinone oxidoreductase, NDH-II ($H^+/e^- = 0$).

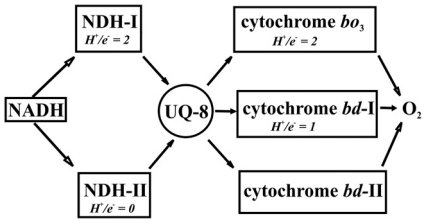

Fig. 1. Scheme of the components of the *E. coli* aerobic respiratory chain, starting with NADH as the substrate. Enzyme bioenergetic efficiency is indicated as the number of protons released into the periplasm per electron (H^+/e^- ratio). NDH-I and NDH-II are the coupled and uncoupled NADH:quinone oxidoreductases, respectively, and UQ-8 is ubiquinone-8. NDH-I and NDH-II transfer electrons to UQ-8 to yield reduced UQ-8. Three quinol:oxygen oxidoreductases, cytochromes bo_3, *bd*-I, *bd*-II, oxidize reduced UQ-8 and reduce O_2 to 2 H_2O.

Under growth conditions with high aeration, cytochrome bo_3 predominates, whereas, under microaerophilic conditions, cytochrome *bd*-I is the predominant respiratory oxygen reductase that is present. Conditions of carbon and phosphate starvation result in the induction of a third respiratory oxygen reductase, cytochrome *bd*-II encoded by *app*BC genes (also called *cyx*AB or *cbd*AB) (12–14). The ability of cytochrome *bd*-II to generate a proton motive force is addressed in the current work.

Whereas cytochrome bo_3 and cytochrome *bd*-I have been extensively studied, very little is known about cytochrome *bd*-II. Cytochrome *bd*-I is a two-subunit enzyme carrying three hemes: b_{558}, b_{595}, and *d* (15–17). The latter two hemes are suggested to compose a unique di-heme site for the capture of O_2 and its reduction to H_2O. Heme *d* plays the major role in O_2 binding and formation of oxygenated intermediates (9, 18–25). In contrast, cytochrome *bd*-II remains poorly studied, but it has been shown that its spectral properties closely resemble those of cytochrome *bd*-I (26). The amino acid sequences of both subunits of cytochrome *bd*-I and *bd*-II are also highly homologous (about 60% identity).

It has been reported recently that cytochrome *bd*-II does not contribute to the generation of the proton motive force ($H^+/e^- = 0$) (27). This was deduced from the growth properties

Author contributions: V.B.B., M.L.V., D.A.B., R.B.G., and M.I.V. designed research; V.B.B., R.M., M.L.V., D.A.B., H.H., and M.I.V. performed research; M.I.V. contributed new reagents/analytic tools; V.B.B., R.M., M.L.V., D.A.B., H.H., R.B.G., and M.I.V. analyzed data; and V.B.B., M.L.V., D.A.B., R.B.G., and M.I.V. wrote the paper.

The authors declare no conflict of interest.

*This Direct Submission article had a prearranged editor.

[1]V.B.B. and R.M. contributed equally to this work.

[2]To whom correspondence should be addressed. E-mail: michael.verkhovsky@helsinki.fi.

of the strain that was genetically constructed to lack NDH-I, cytochrome bo_3 and cytochrome *bd*-I. The aerobic respiratory chain from NADH is constrained to NDH-II → *bd*-II. By examination of the growth of this strain under glucose-limited conditions in continuous culture, it was concluded that cytochrome *bd*-II does not contribute to the proton motive force (i.e., the aerobic respiratory chain is fully uncoupled). Shepherd et al. (28) have proposed that under such conditions *E. coli* creates the proton motive force by means of consumption of intracellular protons during the synthesis of γ-aminobutyric acid (GABA), which is coupled to the electrogenic uptake of anionic glutamate by the glutamate/GABA antiporter.

In this work we directly determined the ability of cytochrome *bd*-II to generate a proton motive force by examining intact cells, spheroplasts, and membrane vesicles as well as purified cytochrome *bd*-II. The data definitively show that the catalytic turnover of cytochrome *bd*-II does generate a proton motive force by a mechanism identical to that of cytochrome *bd*-I. A previous proposal (29) that the *bd*-type oxygen reductase from *Azotobacter vinlandii* is not coupled has also been demonstrated not to be correct (30). It is very likely, therefore, that all members of the family of *bd*-type oxygen reductases generate a proton motive force even as they may have additional roles such as scavenging O_2 or maintaining redox balance in the cytoplasm. The data presented has import in examining the bioenergetics of other organisms which use cytochrome *bd*.

Results

Steady-State Generation of ΔΨ and ΔpH. ΔΨ and ΔpH measurements were performed with inverted membrane vesicles of *E. coli* strain MB37 lacking NDH-I, cytochrome bo_3, and cytochrome *bd*-I. Thus, all three of the known electrogenic components of the aerobic respiratory chain are absent. NADH oxidation can proceed via the NDH-II → *bd*-II branch (Fig. 1). Fig. 2*A* shows that the addition of ATP (trace 1) or the substrate of *bd*-II [Q_1 plus a reductant DTT (trace 2)], results in a spectral shift of oxonol VI, indicating the formation of ΔΨ in the inverted vesicles (inside positive). The ΔΨ is entirely eliminated upon the addition of gramicidin, which creates channels in the membrane. These data show that ΔΨ across the bacterial membrane is generated due to either turnover of the F_1F_O ATPase (trace 1) or by quinol oxidase activity (trace 2). Because the only quinol oxidase present is cytochrome *bd*-II, these data imply that catalytic turnover of cytochrome *bd*-II generates a transmembrane potential (ΔΨ) under steady-state conditions.

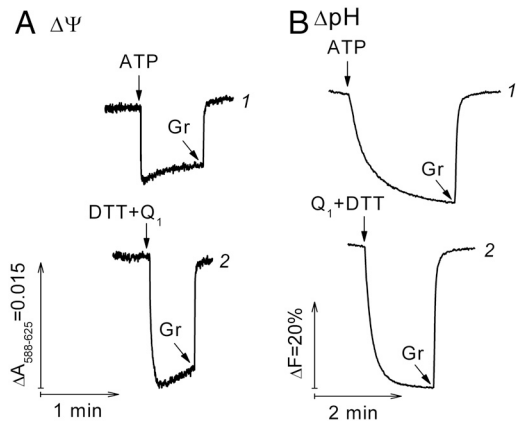

Fig. 2. Steady-state generation of Δ*p* by the inverted membrane vesicles from an *E. coli* strain engineered to contain cytochrome *bd*-II as the only terminal oxidase. (*A*) ΔΨ generation measured with 25 mM HEPES + BIS-TRIS propane at pH 7.5, 1 mM $MgCl_2$, 2 μM oxonol VI, and vesicles (72 μg protein/mL). The arrows show that the reaction was initiated by addition of 1 mM ATP (trace *1*) or 50 μM Q_1 in the presence of 1 mM DTT and 6.25 mM $(NH_4)_2SO_4$ (trace *2*). The ΔΨ was then dissipated by the addition of 1 μg/mL gramicidin (Gr). (*B*) Acidification of the vesicle interior measured with 100 mM HEPES-KOH at pH 7.5, 50 mM K_2SO_4, 5 μM AO, vesicles (36 μg protein/mL), and 1 μM valinomycin. The reaction was initiated by addition of 0.1 mM ATP in the presence of 10 mM $MgSO_4$ (trace *1*) or 1 mM DTT in the presence of 50 μM Q_1 and 1 mM $MgSO_4$ (trace *2*). The generated ΔpH was then dissipated by 1 μg/mL gramicidin (Gr), as indicated by the arrows.

Fig. 2*B* shows the responses of the dye acridine orange (AO) under the same conditions, reporting the internal acidification in the inverted vesicles, and, therefore, formation of ΔpH. The addition of either ATP (trace 1) or Q_1 plus DTT (trace 2) results in quenching of the AO fluorescence, demonstrating acidification of the vesicle interior. These pH changes are abolished by gramicidin. The data clearly show that catalytic turnover of cytochrome *bd*-II is accompanied by the release of protons on the periplasmic side of the membrane, equivalent to the inside of the inverted vesicles.

It is noted that the observed kinetics of the generation of ΔΨ and ΔpH are different (Fig. 2). This is because ΔΨ is produced almost immediately, whereas ΔpH develops at a much slower rate since the membrane vesicles are loaded with concentrated buffer.

H^+/e^- Ratio Measurement. Fig. 3*B* shows the change in the pH of an anaerobic suspension of spheroplasts from *E. coli* MB37 (lacking NDH-I, cytochrome bo_3 and cytochrome *bd*-I) upon addition of aliquots of O_2. By calibrating with HCl, the number of released protons can be calculated as 0.94 ± 0.18 H^+/e^-. The data is an average of nine measurements with two different spheroplasts preparations. As shown in Fig. 3*A*, under identical conditions virtually the same ratio (1.0 ± 0.07 H^+/e^-) can be obtained with spheroplasts from strain MB30, in which NDH-I, cytochrome bo_3, and cytochrome *bd*-II have all been removed. The only

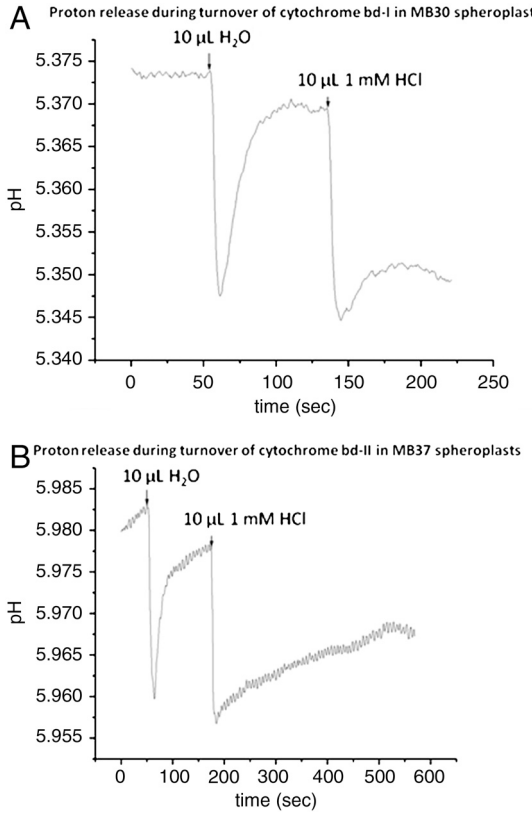

Fig. 3. Proton release from spheroplasts prepared from (*A*) *E. coli* strain MB30 [Δ*cyoB* Δ*appB* Δ*nuoB*] in which cytochrome *bd*-I is the only terminal oxidase present; and (*B*) *E. coli* strain MB37 [Δ*cyoB* Δ*cydB* Δ*nuoB*] in which cytochrome *bd*-II is the only terminal oxidase present. For conditions, see the text. O_2 was added as air-saturated water (25 °C, 1 atm).

possible source of released protons in strain MB30 is cytochrome *bd*-I. This data is an average of 12 measurements with two different spheroplast preparations. The H^+/e^- stoichiometry for cytochrome *bd*-I is in agreement with that reported earlier (5). O_2 pulses were also performed with whole cells at pH 7.3 and the results are the same as with the spheroplasts at pH 5.0. The proton release from spheroplasts, by either cytochrome *bd*-I or cytochrome *bd*-II, is inhibited by the addition of aurachin (C1-10), an inhibitor of the quinol oxidases.

Single-Turnover Generation of Membrane Potential. Fig. 4 shows the time course of single-turnover $\Delta\Psi$ generation by the liposome-incorporated, fully reduced cytochrome *bd*-II during its reaction with O_2. The electrometric kinetics consists of an initial lag-phase reflecting a nonelectrogenic process, followed by an electrogenic phase. Fitting the kinetics with a sequential-step reaction model (31) gives two electrically silent steps with time constants (τ) of 2.1 and 7.3 μs, respectively, for the lag phase, and two steps with τ of 70 μs and 440 μs and with their relative amplitudes of approximately 90% and 10%, respectively, for the electrogenic phase. Similar kinetics of $\Delta\Psi$ generation by cytochrome *bd*-I has been demonstrated previously under the same conditions (10). In the latter work, based also on the concomitant time-resolved optical measurements, the two nonelectrogenic steps have been correlated to the transition from the reduced heme *d* (state **R**) to the heme *d* oxy-complex (state **A**) followed by the formation of the heme *d* peroxy complex (state **P**). The two electrogenic steps correlate with the sequential conversion of the peroxy intermediate to the ferryl species (state **F**) and then to the oxidized species (state **O**). Note that the **F** → **O** transition occurs only in a small fraction of the enzyme that contains bound quinol. For this reason, this reaction is associated with a relatively small electrogenic amplitude (10% of the total voltage). The data demonstrate that the two enzymes, *bd*-I and *bd*-II, function in the same manner.

Discussion

The current work was inspired by the report by Bekker et al. (27) concerning the function of cytochrome *bd*-II in the *E. coli* aerobic respiratory chain. By constructing a strain (MB37; *cyo, cyd, nuo*) in which the only terminal oxidase is cytochrome *bd*-II, aerobic respiration utilizing this enzyme was clearly demonstrated and quantified during continuous culture under glucose-limited growth conditions. If all three terminal oxygen reductases were absent, no oxygen utilization was observed and the strain (MB44) grows by homolactate fermentation (27). Despite the fact that the strain in which cytochrome *bd*-II is the only terminal oxidase consumes oxygen, a detailed analysis resulted in the conclusion that cytochrome *bd*-II does not contribute to the proton motive force (27). Hence, according to these data, strain MB37 lacks all three of the respiratory components that contribute to the proton motive force, leaving open the question of how ATP is generated. Substrate-level phosphorylation was suggested (27) and, subsequently, it was suggested that a proton motive force could be generated by the operation of an electrogenic antiporter that imports anionic glutamate and exports newly synthesized, neutral GABA (28). According to this interpretation, *E. coli* cells have the capacity to insert into its respiratory chain a terminal oxidase that is maximally coupled to the generation of the proton motive force (bo_3 : $H^+/e^- = 2$), minimally coupled (*bd*-II : $H^+/e^- = 0$), or intermediate (*bd*-I: $H^+/e^- = 1$), depending on the physiological need.

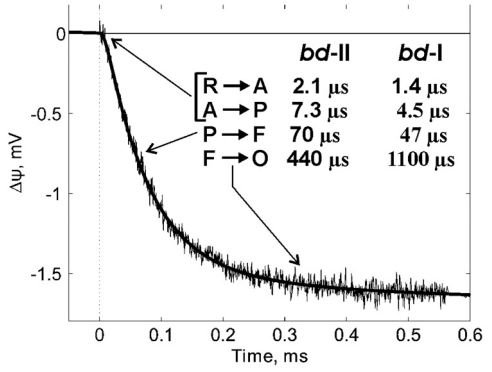

Fig. 4. Single-turnover generation of the transmembrane electric potential during the reaction of the fully reduced, reconstituted cytochrome *bd*-II from *E. coli* with O_2. Conditions: 100 mM MOPS-KOH at pH 7.2, 10 μM hexaammineruthenium, 5 μM *N,N,N′,N′*-tetramethyl-*p*-phenylendiamine, 50 mM glucose, 0.5 mg/mL catalase, 1.5 mg/mL glucose oxidase and 1% CO. The reaction was started by a laser flash (time = 0, indicated by a dashed line) 400 ms following the injection of 50 μL of oxygen-saturated buffer ($[O_2]$ = 1.2 mM) at 21 °C. The fit line is a best fit result for a consecutive-step reaction model with two lag-phases (electrically silent steps, τ, 2.1 μs and 7.3 μs, respectively) and two $\Delta\Psi$ generation steps (τ, 70 μs, and contribution, 90%, and τ, 440 μs, and contribution, 10%, respectively). The respective phases are indicated by arrows. The time constants for *bd*-I are taken from ref. 10.

In the current work, the ability of cytochrome *bd*-II to generate a proton motive force was directly measured. Contrary to the expectation based on the continuous culture experiments (27), it is definitively shown that catalytic turnover of cytochrome *bd*-II does generate a proton motive force. Steady-state ubiquinol-1 oxidase activity by inverted vesicles of strain MB37, in which cytochrome *bd*-II is the only quinol oxidase, is coupled to the generation of both the $\Delta\Psi$ and ΔpH components of proton motive force (Fig. 2). Because inverted vesicles from this strain also contain a well-coupled F_0F_1-ATPase, both $\Delta\Psi$ (Fig. 2*A*, trace 1) and ΔpH (Fig. 2*B*, trace 1) can also be generated by addition of ATP. Hence, in the MB37 cells, aerobic respiration must be coupled to ATP synthesis via the cytochrome *bd*-II terminal oxidase.

We also determined the bioenergetic efficiency (i.e., H^+/e^- ratio) of the aerobic respiratory chain using MB37 spheroplasts (Fig. 3*B*), as well as whole cells, by measuring protons released during steady-state turnover using endogenous substrates. Because this strain also lacks the coupled NDH-I (NADH: ubiquinone oxidoreductase), this effectively measures the proton release from cytochrome *bd*-II. The data show that each electron used to reduce O_2 results in the release of one proton ($H^+/e^- = 1$). The same result was obtained with cytochrome *bd*-I (Fig. 3*A*) but is half the value reported previously for cytochrome bo_3 (5), which is a proton pump. Hence, these data indicate that cytochrome *bd*-II, like cytochrome *bd*-I, is not a proton pump. The scheme in Fig. 5 shows how this stoichiometry is attained. Charge separation accompanies catalytic turnover of the enzyme because the electrons and protons used to reduce O_2 to 2 H_2O come from opposite sides of the membrane. Quinol is oxidized at a site near the periplasmic surface, releasing protons into the periplasm. The protons used to form H_2O are taken from the cytoplasm delivered across the membrane by a putative proton conducting channel.

Single-turnover electrometric experiments with the purified cytochrome *bd*-II incorporated in proteoliposomes allowed us to elucidate which of the partial reactions in the catalytic cycle are coupled to the generation of membrane potential. The $\Delta\Psi$ transient caused by the reaction of the fully reduced cytochrome *bd*-II with O_2 consists of an initial, nonelectrogenic part (the lag-phase) followed by the electrogenic part (Fig. 4). The lag-phase is the sum of the two faster, nonelectrogenic processes and the electrogenic part consists of two slower electrogenic transitions with the first phase contributing the most to the $\Delta\Psi$. The phases and rate constants are similar to those measured for cytochrome *bd*-I (10). Therefore by analogy, it is proposed that the four phases observed with cytochrome *bd*-II correspond to the **R** → **A**, **A** → **P**, **P** → **F**, and **F** → **O** transitions, respectively,

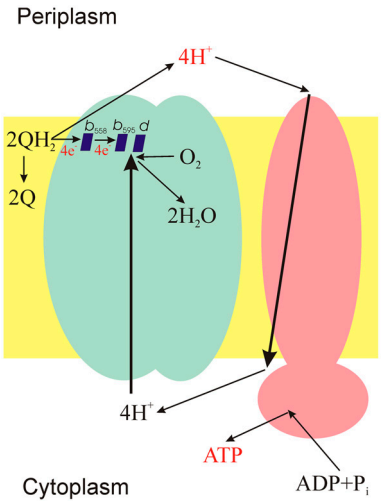

Fig. 5. Schematic model of coupling between respiration and phosphorylation in *E. coli* in which the aerobic respiratory chain in which cytochrome *bd*-II is the only site that can generate a proton motive force. Shown are cytochrome *bd*-II (green) and the F_1F_O-ATP synthase (pink) embedded in the cytoplasmic membrane (yellow). The same diagram applies also to cytochrome *bd*-I. The proton motive force is composed of two components that depend on the magnitude of the transmembrane electric potential difference ($\Delta\Psi$) and the pH gradient across the membrane. In vivo, the pH gradient is determined by the buffering of the external environment and by pH homeostasis mechanisms to control the internal pH. In inverted membrane vesicles, the small internal volume is readily acidified by proton release from the oxidation of ubiquinol. The transmembrane potential is postulated to be formed by the vectorial uptake of protons from the cytoplasmic side of the membrane to the di-heme (b_{595}-*d*) active site to form water. The resulting proton motive force is used by the F_1F_O-ATP synthase to produce ATP from ADP and inorganic phosphate.

and that the membrane potential is produced during the last two transitions—i.e., the conversion of the peroxy intermediate to the ferryl species and during the further transition of the ferryl to the oxidized species.

The present study strongly suggests that the mechanism of cytochrome *bd*-II is identical to that of cytochrome *bd*-I, which is consistent with the strong sequence homology of the two enzymes. It is concluded that cytochrome *bd*-II is a primary generator of the proton motive force and, therefore, alternate mechanisms for the generation of ATP (27, 28) are not required to explain the growth of strain MB37 (*nuo, cyo, cyd*).

Materials and Methods

Cell Culture. The *E. coli* strains MB37 (BW25113 Δ*cyoB* Δ*cydB* Δ*nuoB*, kanamycin marker removed) and MB30 (BW25113 Δ*cyoB* Δ*appB* Δ*nuoB*, kanamycin marker removed) containing cytochrome *bd*-II and cytochrome *bd*-I as the sole terminal oxidase, respectively (27), were a kind gift of M. Bekker (University of Amsterdam). The cells were grown aerobically in a 25 L fermentor with stirring (at aeration rate of 20 L/min) or in flasks on a shaker (at 200 rpm) in LB medium at 37 °C for 4–5 hrs until the late exponential phase.

Enzyme Isolation. Cytochrome *bd*-II was purified following a protocol described for cytochrome *bd*-I (32), with modifications. The MB37 membranes were solubilized with sucrose monolaurate (1.8% final concentration). After solubilization, the membranes were centrifuged (160,000 g × 60 min, 4 °C), the pellet was discarded and the supernatant loaded on a DEAE-Sepharose Fast Flow column equilibrated with 50 mM potassium phosphate buffer also containing 25 mM KCl, 5 mM EDTA, and 0.1% sucrose monolaurate, pH 6.5. The elution was performed with a KCl gradient (25–470 mM). The fractions with an absorbance ratio of $A_{412}/A_{280} \geq 0.7$ were collected and concentrated.

Steady-State Generation of ΔΨ and ΔpH. For these measurements, inverted membrane vesicles were prepared. The cells were converted into spheroplasts by treatment with 0.1 mg/mL lysozyme in 200 mM Tris-HCl, 2 mM EDTA at pH 8.0, and 30% sucrose. The spheroplasts were pelleted at 5,000 g× 10 min, suspended in 100 mM HEPES-KOH, 50 mM K_2SO_4, 10 mM $MgSO_4$ at pH 7.5, 2 mM dithiotreitol (DTT), and 0.5 mM phenylmethanesulfonyl fluoride and sonicated. The cell debris was removed by centrifugation (at 5,000 × *g* for 10 min). The supernatant was ultracentrifuged at 120,000 × *g* for 30 min. The membrane vesicles were suspended in 25 mM HEPES + BIS-TRIS propane at pH 7.5 and used the same day. Steady-state generation of ΔΨ by the vesicles was monitored by the spectral shift of the lipophilic anionic dye oxonol VI. The absorption changes were followed in dual wavelength kinetics mode (588–625 nm) using a Shimadzu UV-3000 spectrophotometer. Acidification of the interior of the vesicles was followed by quenching of fluorescence of the pH-sensitive membrane-permeable dye AO. Measurements were carried out at 21 °C using a Hitachi F-4000 fluorescence spectrophotometer using 493 nm (excitation) and 530 nm (emission). The response was expressed as the percentage of the fluorescence intensity before addition of the substrate.

Measurement of H^+/e^- Ratio. The measurement was performed both with spheroplasts and intact cells. Spheroplasts were prepared using lysozyme and EDTA as in ref. 33, collected by centrifugation and then resuspended in 0.5 mM HEPES-KOH at pH 5.0, 100 mM KSCN, and 150 mM KCl. Then spheroplasts were pelleted once again and resuspended in the same medium. Proton release by whole cells was studied at pH 7.3, whereas experiments with spheroplasts were performed at the pH value of 5.0 to optimize their stability (34). The results were similar whether intact cells or spheroplasts were examined. Spheroplasts were used to determine if the proton translocation and oxidase activities were inhibited by aurachin (C1-10), a potent inhibitor of cytochrome *bd*-I (35, 36) that does not readily penetrate the outer membrane of intact cells. Proton release by spheroplasts was measured as follows. The spheroplast suspension (100 μL) was diluted into 2.5 mL of 0.5 mM HEPES-KOH at pH 5.0, 100 mM KSCN, and 150 mM KCl. Dissolved oxygen was removed by passing a stream of water-saturated argon over the solution in a sealed chamber (at 25 °C) equipped with a glass pH-electrode (Thermo Russell pH electrode, type CMAW711). Traces of oxygen were removed from the solution by letting the spheroplasts respire with endogenous substrates. Endogenous substrates are also responsible for the respiration during the oxygen pulse used to measure the proton release. To measure the H^+/e^- ratio, 10 μL of air-saturated water (250 μM) was injected into the solution and the pH change was recorded. After reequilibration, 10 μL of a 1 mM HCl solution was injected into the sample and the pH change was recorded as a calibration of the system. The number of protons ejected from the spheroplasts upon the reduction of O_2 contained in 10 μL of air-saturated water (250 pmole/μL) was calculated by noting the amount of HCl required to elicit the same change in pH. The addition of aurachin (C1-10) to a final concentration of 80 μM eliminated proton translocation for both cytochrome *bd*-I and cytochrome *bd*-II in the spheroplast preparations.

Oxidase Activity Assay. Oxidase activity was measured by monitoring the depletion of dissolved oxygen as a function of time using a Clark-type electrode (YSI Inc.) at 37 °C after the addition of 100 μL of a suspension of either whole cells or spheroplasts to 1.7 mL of the same buffer used for proton-pumping measurements.

Single-Turnover Generation of ΔΨ. Reconstitution of cytochrome *bd*-II into liposomes, preparation of the anaerobic samples, and the direct electrometric measurements with a microsecond time resolution were performed essentially as reported (refs. 8–11 and references therein).

Heme and Protein Concentration. The heme *d* content was measured from the reduced-*minus*-"air-oxidized" difference absorption spectra using $\Delta\epsilon_{628-607}$ of 10.8 $mM^{-1}\,cm^{-1}$ (20). Protein concentration was determined by the BCA Protein Assay Reagent kit (Pierce) with bovine serum albumin as a standard.

Data Analysis. MATLAB (The Mathworks) and Origin (OriginLab Corporation) were used for data manipulation and presentation.

ACKNOWLEDGMENTS. We thank Dr. M. Bekker (University of Amsterdam) for providing the strains of *E. coli* MB37 and MB30 and Ms. V. Rauhamäki (University of Helsinki) for her assistance with growing the *E. coli* cells. This work was supported by the Russian Foundation for Basic Research (to V.B.B., Grant 11-04-00031-a), the National Institutes of Health (to R.B.G., Grant HL16101), and Biocentrum Helsinki, Sigrid Jusélius Foundation, Magnus Ehrnrooth Foundation, and the Academy of Finland (to M.I.V., M.L.V., and D.A.B.).

1. Poole RK, Cook GM (2000) Redundancy of aerobic respiratory chains in bacteria? Routes, reasons and regulation. *Adv Microb Physiol* 43:165–224.
2. Bogachev AV, Murtazina RA, Skulachev VP (1996) H^+/e^- stoichiometry for NADH dehydrogenase I and dimethyl sulfoxide reductase in anaerobically grown *Escherichia coli* cells. *J Bacteriol* 178:6233–6237.
3. Puustinen A, Finel M, Virkki M, Wikström M (1989) Cytochrome *o* (*bo*) is a proton pump in *Paracoccus denitrificans* and *Escherichia coli*. *FEBS Lett* 249:163–167.
4. Anraku Y, Gennis RB (1987) The aerobic respiratory chain of *Escherichia coli*. *Trends Biochem Sci* 12:262–266.
5. Puustinen A, Finel M, Haltia T, Gennis RB, Wikström M (1991) Properties of the two terminal oxidases of *Escherichia coli*. *Biochemistry* 30:3936–3942.
6. Mogi T, et al. (1998) Two terminal quinol oxidase families in *Escherichia coli*: Variations on molecular machinery for dioxygen reduction. *J Biochem Mol Biol Biophys* 2:79–110.
7. Borisov VB, Verkhovsky MI (2009) *EcoSal: Escherichia coli and Salmonella: Cellular and Molecular Biology*, eds A Böck et al. (ASM Press, Washington, DC), http://www.ecosal.org; chapter 3.2.7.
8. Jasaitis A, et al. (2000) Electrogenic reactions of cytochrome *bd*. *Biochemistry* 39:13800–13809.
9. Belevich I, et al. (2005) Time-resolved electrometric and optical studies on cytochrome *bd* suggest a mechanism of electron-proton coupling in the di-heme active site. *Proc Natl Acad Sci USA* 102:3657–3662.
10. Belevich I, Borisov VB, Verkhovsky MI (2007) Discovery of the true peroxy intermediate in the catalytic cycle of terminal oxidases by real-time measurement. *J Biol Chem* 282:28514–28519.
11. Borisov VB, Belevich I, Bloch DA, Mogi T, Verkhovsky MI (2008) Glutamate 107 in subunit I of cytochrome *bd* from *Escherichia coli* is part of a transmembrane intraprotein pathway conducting protons from the cytoplasm to the heme *b*595/heme *d* active site. *Biochemistry* 47:7907–7914.
12. Dassa J, et al. (1991) A new oxygen-regulated operon in *Escherichia coli* comprises the genes for a putative third cytochrome oxidase and for pH 2.5 acid phosphatase (appA). *Mol Gen Genet* 229:341–352.
13. Atlung T, Brøndsted L (1994) Role of the transcriptional activator AppY in regulation of the *cyx appA* operon of *Escherichia coli* by anaerobiosis, phosphate starvation, and growth phase. *J Bacteriol* 176:5414–5422.
14. Brøndsted L, Atlung T (1996) Effect of growth conditions on expression of the acid phosphatase (*cyx-appA*) operon and the *appY* gene, which encodes a transcriptional activator of *Escherichia coli*. *J Bacteriol* 178:1556–1564.
15. Trumpower BL, Gennis RB (1994) Energy transduction by cytochrome complexes in mitochondrial and bacterial respiration: The enzymology of coupling electron transfer reactions to transmembrane proton translocation. *Annu Rev Biochem* 63:675–716.
16. Borisov VB (1996) Cytochrome *bd*: Structure and properties. *Biochemistry (Moscow)* 61:565–574 (translated from *Biokhimiya* (in Russian) (1996) 61:786–799.
17. Jünemann S (1997) Cytochrome *bd* terminal oxidase. *Biochim Biophys Acta* 1321:107–127.
18. Hill JJ, Alben JO, Gennis RB (1993) Spectroscopic evidence for a heme-heme binuclear center in the cytochrome *bd* ubiquinol oxidase from *Escherichia coli*. *Proc Natl Acad Sci USA* 90:5863–5867.
19. Tsubaki M, Hori H, Mogi T, Anraku Y (1995) Cyanide-binding site of *bd*-type ubiquinol oxidase from *Escherichia coli*. *J Biol Chem* 270:28565–28569.
20. Borisov V, Arutyunyan AM, Osborne JP, Gennis RB, Konstantinov AA (1999) Magnetic circular dichroism used to examine the interaction of *Escherichia coli* cytochrome *bd* with ligands. *Biochemistry* 38:740–750.
21. Vos MH, Borisov VB, Liebl U, Martin J-L, Konstantinov AA (2000) Femtosecond resolution of ligand-heme interactions in the high-affinity quinol oxidase *bd*: A di-heme active site? *Proc Natl Acad Sci USA* 97:1554–1559.
22. Borisov VB, Sedelnikova SE, Poole RK, Konstantinov AA (2001) Interaction of cytochrome *bd* with carbon monoxide at low and room temperatures: Evidence that only a small fraction of heme *b*595 reacts with CO. *J Biol Chem* 276:22095–22099.
23. Borisov VB, et al. (2002) Interactions between heme *d* and heme *b*595 in quinol oxidase *bd* from *Escherichia coli*: A photoselection study using femtosecond spectroscopy. *Biochemistry* 41:1654–1662.
24. Arutyunyan AM, et al. (2008) Strong excitonic interactions in the oxygen-reducing site of *bd*-type oxidase: The Fe-to-Fe distance between hemes *d* and *b*595 is 10 Å. *Biochemistry* 47:1752–1759.
25. Rappaport F, Zhang J, Vos MH, Gennis RB, Borisov VB (2010) Heme-heme and heme-ligand interactions in the di-heme oxygen-reducing site of cytochrome *bd* from *Escherichia coli* revealed by nanosecond absorption spectroscopy. *Biochim Biophys Acta* 1797:1657–1664.
26. Sturr MG, Krulwich TA, Hicks DB (1996) Purification of a cytochrome *bd* terminal oxidase encoded by the *Escherichia coli* app locus from a Δ*cyo* Δ*cyd* strain complemented by genes from *Bacillus firmus* OF4. *J Bacteriol* 176:1742–1749.
27. Bekker M, de Vries S, Ter Beek A, Hellingwerf KJ, de Mattos MJ (2009) Respiration of *Escherichia coli* can be fully uncoupled via the nonelectrogenic terminal cytochrome *bd*-II oxidase. *J Bacteriol* 191:5510–5517.
28. Shepherd M, Sanguinetti G, Cook GM, Poole RK (2010) Compensations for diminished terminal oxidase activity in *Escherichia coli*: Cytochrome *bd*-II-mediated respiration and glutamate metabolism. *J Biol Chem* 285:18464–18472.
29. Ackrell BA, Jones CW (1971) The respiratory system of *Azotobacter vinelandii*. 1. Properties of phosphorylating respiratory membranes. *Eur J Biochem* 20:22–28.
30. Bertsova YV, Bogachev AV, Skulachev VP (1997) Generation of protonic potential by the *bd*-type quinol oxidase of *Azotobacter vinelandii*. *FEBS Lett* 414:369–372.
31. Bloch DA, Jasaitis A, Verkhovsky MI (2009) Elevated proton leak of the intermediate O_H in cytochrome *c* oxidase. *Biophys J* 96:4733–4742.
32. Borisov VB (2008) Interaction of *bd*-type quinol oxidase from *Escherichia coli* and carbon monoxide: Heme *d* binds CO with high affinity. *Biochemistry (Moscow)* 73:14–22 (translated from *Biokhimiya* (in Russian) (2008) 73:18–28.
33. Sullivan CJ, Morrell JL, Allison DP, Doktycz MJ (2005) Mounting of *Escherichia coli* spheroplasts for AFM imaging. *Ultramicroscopy* 105:96–102.
34. Edebo L (1961) Lysis of bacteria. 3. On the stability of protoplasts and spheroplasts in different pH-ranges. *Acta Pathol Microbiol Scand* 53:121–128.
35. Miyoshi H, Takegami K, Sakamoto K, Mogi T, Iwamura H (1999) Characterization of the ubiquinol oxidation sites in cytochromes *bo* and *bd* from *Escherichia coli* using aurachin C analogues. *J Biochem* 125:138–142.
36. Jünemann S, Wrigglesworth JM, Rich PR (1997) Effects of *decyl*-aurachin D and reversed electron transfer in cytochrome *bd*. *Biochemistry* 36:9323–9331.